https://doi.org/10.5194/egusphere-2025-5616
Preprint. Discussion started: 20 November 2025

Manuscript submitted to Geophysical Journal International (Express Letter)

Spherical Harmonic Analogues: robust measures of palaeomagnetic field behaviour obtained using an ensemble of geodynamo simulations

Andrew J. Biggin

Geomagnetism Laboratory, School of Environmental Sciences, University of Liverpool, UK.

Email: biggin@liverpool.ac.uk

Summary

The palaeomagnetic field provides unique information about the deep Earth and allows past plate motions and true polar wander to be determined. While data are available across much of Earth's history, the conversion of these into robust descriptions of palaeomagnetic field behaviour prior to 1 Ma has been hampered by their highly inhomogeneous distributions in space and time. To address this, a set of parameters termed *spherical harmonic analogues* are proposed that use robust statistics to capture global, time-averaged aspects of field behaviour. Global palaeomagnetic direction and intensity data may be combined with outputs from ensembles of numerical geodynamo simulations, using a bespoke Monte-Carlo proxy-based approach, to estimate values of these spherical harmonic analogues using data from long before 1 Ma. The new approach is applied to the intervals 0.1-1 Ma, 1-4 Ma, and 4-15 Ma which were chosen for the

https://doi.org/10.5194/egusphere-2025-5616
Preprint. Discussion started: 20 November 2025

moderately uniform distributions of the ages of data within them. The resulting estimates account for measurement errors and spatial inhomogeneity in the data and perform well in independent validation tests. They therefore provide benchmarks against which statistical field models and geodynamo simulations may be compared. Obtained values suggest that the average axial and nonaxial dipole fields in the interval 0.1-1 Ma were ~50% higher than long-term averages estimated for the preceding 14 million years. By contrast, the time-variance of the total field may have remained relatively constant over the entire interval providing a potential explanation for why the Bruhnes polarity chron is already one of the longest since 15 Ma.

Keywords: Palaeomagnetism; Palaeointensity; Palaeomagnetic secular variation; Dynamo: theories and simulations; Reversals: process, time scale, magnetostratigraphy.

1. Introduction

Global palaeomagnetic datasets comprise many thousands of high-quality measurements of the local direction and / or intensity of the ancient magnetic field tied to independently obtained age estimates that span most of geological history. Their limited spatiotemporal distribution has, however, restricted published geomagnetic field models (e.g. Mahgoub *et al.*, 2023, Panovska *et al.*, 2018, Pavon-Carrasco *et al.*, 2014), that utilise more than a single time-varying spherical harmonic term, to specific intervals within the last million years. For earlier times, models either define only the axial dipole field (ADF; e.g. Bono *et al.*, 2022, Ziegler *et al.*, 2011) or are entirely

https://doi.org/10.5194/egusphere-2025-5616
Preprint. Discussion started: 20 November 2025

statistical in nature. Models based on a giant Gaussian process (GGP; e.g. Bono *et al.*, 2020, Tauxe *et al.*, 2024) are instructive but, while they purport to represent the global field across the entire time period from which the data constraining them are sourced, these measurements may be distributed in a highly non-uniform manner in time and space. The potential exists therefore for models to be very strongly influenced by field behaviour in certain regions and during specific sub-intervals of time. As an illustrative example, ~48% of directional data and ~69% of intensity data used to constrain the BB18 model for 0-10 Ma were from rocks from the 0-1 Ma time period and ~85% of the palaeointensities were from northern hemisphere sites.

This study outlines a new approach for characterising average properties of ancient magnetic field behaviour in time intervals times that are too old for time-varying spherical harmonic models to be viable. It is designed to account for the inherently sparse and unevenly distributed nature of palaeomagnetic datasets and deliver a useful set of descriptive parameters – termed *spherical harmonic analogues* (SHAnalogues from hereon) – accompanied by realistic uncertainty bounds. This paper will first define the SHAnalogues themselves and then outline the method for obtaining them from palaeomagnetic datasets and validating their accuracy. The approach is applied to data from three time-intervals within 0-15 Ma and the results discussed.

2. Spherical Harmonic Analogues

https://doi.org/10.5194/egusphere-2025-5616
Preprint. Discussion started: 20 November 2025

We consider the internally-sourced geomagnetic field at Earth's surface expressed as a series of Gauss coefficients using the very well-established approach outlined by e.g. Stacey (1992). The root-mean-square field strength due to a single Gauss coefficient is:

$$(B_l^m)_{rms} = (l+1)^{1/2}\left(g_l^m, h_l^m\right) \qquad (1)$$

Where g_l^m andh_l^m are Gauss coefficients, calculated at Earth's surface, of degree *l* and order *m*.

The strengths of the axial dipole field (*ADF*) and total field (*TF*) are then:

$$ADF = (B_1^0)_{rms} \qquad (2)$$

$$TF = \left[\sum_{l=1}^{10} R_l\right]^{1/2} \qquad (3)$$

where:

$$R_l = (l+1)\sum_{m=0}^{l}\left[\left(g_l^m\right)^2 + (h_l^m)^2\right] \qquad (4)$$

All terms other than g_1^0 comprise the non-axial dipole field whose strength (*NADF*) is determined from equations (3) and (4), after setting g_1^0 to zero:

$$NADF = TF|_{g_1^0=0} \qquad (5)$$

https://doi.org/10.5194/egusphere-2025-5616
Preprint. Discussion started: 20 November 2025

Time series of Gauss coefficients at Earth's surface output by geomagnetic field models and geodynamo simulations are truncated at degree and order 10 and used to calculate *ADF*, *NADF* and *TF* at each time step. Subsequently, ADF_{median}, $NADF_{median}$, and TF_{iqr} are calculated as measures of their time averages (medians) and variance (interquartile range, *iqr*). As summarised and exemplified in figure 1, the four SHAnalogues introduced here comprise: the two time averaged field intensities ADF_{median} *and* $NADF_{median}$; the square-root of the ratio of these $(NADF_{median} / ADF_{median})^{1/2}$ which describes the typical spatial complexity of the field and is referred to as *Roughness;* and the square-root of the ratio of the total-field variance to the median of the axial dipole field $(TF_{iqr} / ADF_{median})^{1/2}$ which describes the temporal complexity of the field and is referred to as *Volatility*. Clearly, alternative means of parameterising similar summary information to those outlined here exist. These specific parameters were chosen because: (1) robust statistics (in place of means and standard deviations) prevent outliers from influencing the values; (2) while only ADF_{median}, *Roughness*, and *Volatility* may be estimated directly from palaeomagnetic data (see below), defining them in this way does allow $NADF_{median}$ and TF_{iqr} to be calculated subsequently; (3) the incorporation of square-roots allows values of *Roughness* and *Volatility* values obtained from diverse models to be compared conveniently on plots with linear axes.

<Figure 1>

Figure 1 illustrates the SHAnalogues derived from two time-varying field models (Mahgoub *et al.*, 2023, Panovska *et al.*, 2018) and Table S1 provides the values obtained from a further 9 field

https://doi.org/10.5194/egusphere-2025-5616
Preprint. Discussion started: 20 November 2025

models used in the analyses to follow (Bono *et al.*, 2020, Brown *et al.*, 2018, Nilsson *et al.*, 2022, Panovska *et al.*, 2021, Schanner *et al.*, 2022, Tauxe *et al.*, 2024, Tauxe and Kent, 2004). The field models, drawn from intervals between 0.009 and 17 million years in duration, yield moderately broad ranges of values. Those values of *Volatility* derived from longer-duration models, tending to cover older time periods, are associated with higher values.

Table S2 provides the input and output parameters (including SHAnalogues) for 57 published geodynamo simulations to be further used in this study but which are described fully elsewhere (Biggin *et al.*, 2025, Meduri *et al.*, 2021, Mound and Davies, 2023). Realisations of geodynamo simulations, spanning ~ 0.05 – to 86 million years, are drawn from models with a very wide range of input parameters exhibiting a correspondingly wide range of behaviours. They may be subdivided into 10 groups (Table S2) within which only the Rayleigh number is varied. This provides ranges of SHAnalogue values that encompass those of the field models. It is highlighted that the exact values of ADF_{median} *and* $NADF_{median}$ are a function of scaling factors that may not be well-constrained and so it is recommended that direct comparisons with observation-based estimates should focus on *Roughness* and *Volatility*. The relationship between the values of SHAnalogues obtained from realisations and their durations appears very weak (figure S1) but it should be remembered that shorter realisations may be less representative of the long-term behaviour.

https://doi.org/10.5194/egusphere-2025-5616
Preprint. Discussion started: 20 November 2025

SHAnalogues provide a convenient means to compare models and simulations but their greatest utility is that they may be estimated directly from palaeomagnetic datasets in a manner that accounts for uneven spatial distributions and measurement errors and yields uncertainty estimates that may then be independently tested. This is achieved through using three measurable palaeomagnetic statistics as proxies for three of the SHAnalogues. The relationship between each proxy and its SHAnalogue, obtained specifically for that spatial distribution of data and the associated measurement errors, is then estimated using a Monte Carlo approach that "down-samples" an ensemble of geodynamo simulation outputs.

The efficacies of three proxies were trialled for each of the three SHAnalogues using several different generic spatial distributions of 100 data. These distributions were chosen to represent extremes of 5 site mean palaeomagnetic measurements at each of 20 different locations, the exact inverse (20 measurements at 5 locations), and a balance of 10 measurements at 10 locations. For each of 10 downsamples per simulation, the locations were randomised, but a uniform spacing of locations was maintained. For ADF_{median}, all trialled proxies performed very well ($R^2 \geq 0.98$, using a linear fit; figure S2). The median VADM, calculated using the actual (palaeo)latitude, was selected as the preferred proxy because it marginally outperformed the others (median VDM and VADM calculated using the associated inclinations) but also, crucially, because it can be calculated from intensity-only data.

https://doi.org/10.5194/egusphere-2025-5616
Preprint. Discussion started: 20 November 2025

It was already established by Biggin *et al*. (2020) that the dispersion of virtual geomagnetic poles (VGPs), derived from low-latitude sites, around their mean position can be used to estimate the axial dipole dominance of the ancient field. The three proxies trialled for *Roughness* followed this premise but were based on the average colatitude of a collection of VGPs (i.e. dispersion around the geographic pole) to avoid the need to group data, measure mean pole positions, or exclude data derived from sites not at low latitudes. The mean VGP colatitude (with and without a 45° cutoff) scaled nonlinearly with *Roughness* at higher values. By contrast, the preferred proxy of median VGP colatitude scaled linearly for all tested values with $R^2 \geq 0.95$ (figure S3).

Proxies for *Volatility* consisted of ratios of the interquartile range and median of collections of V(A)DMs. Relationships were near-linear but somewhat noisier than for other SHAnalogues (R^2 ~ 0.85-088; figure S4). $VADM_{iqr}/VADM_{median}$ was preferred as the marginal best performer and also since it can be calculated from intensity-only measurements.

3. SHAnalogue estimation and testing

The entire process used for estimating and validating SHAnalogues from palaeomagnetic datasets is outlined below using the time interval 0.1-1 Ma as an example.

Step 1: Dataset selection. A time interval was chosen such that > 100 site-mean palaeomagnetic directions and absolute intensities were dated to within it. Any plate motion or

https://doi.org/10.5194/egusphere-2025-5616
Preprint. Discussion started: 20 November 2025

true polar wander occurring since the acquisition of the data was corrected for and, it was checked that both datasets were drawn from reasonably widely distributed regions on the globe. The two datasets were partially independent and, crucially, were not strongly non-uniformly distributed in time. The 0.1-1 Ma directional dataset was drawn from PSV10-24 (Tauxe *et al.*, 2024) after filtering for age and ensuring that each site mean comprised at least 5 samples and an associated precision parameter (*k*) of 50. Associated palaeointensities from this time interval were taken from PINTv8.2 (Chen *et al.*, 2025) requiring a minimum of 3 samples per site and that at least 3 Q_{PI} criteria (Biggin and Paterson, 2014) were met including ALT and MD. The resulting datasets (figure S2) comprised 544 and 190 site-mean directions and intensities respectively with even the latter derived from at least 15 distinct locations with presence on all continents and in the Pacific. The *Gplates* software, utilising the Muller *et al.* (2019) plate model applied in the rotational reference frame, was used to correct site locations and declinations for (very small) motions occurring since formation.

Step 2: Obtained proxies values. VGPs and VADMs were recalculated using updated site locations and palaeomagnetic declinations. The median VGP colatitude, median VADM, and the IQR of the VADMs were then calculated from the datasets with 95% uncertainties estimated using 10,000 bootstraps with resampling. These are shown for 0.1-1 Ma in figure 2.

<***Figure 2***>

https://doi.org/10.5194/egusphere-2025-5616
Preprint. Discussion started: 20 November 2025

Step 3: Obtained ranges of plausible proxy values from down-sampled simulations. For each palaeomagnetic site-mean measurement in both of the datasets:

a. A random timestep within the duration of a geodynamo simulation (drawn from Table S2) was generated from a uniform distribution.
b. The magnetic field vector at the location of the real measurement was calculated using the Gauss coefficients at that timestep
c. A synthetic palaeomagnetic direction or intensity was generated by adding random noise according to the reported site mean statistics. For each directional site mean, this was achieved by first sampling the reported number of samples measurements drawn at random from a Fisher distribution with dispersion parameter κ equal to the reported k. These were then averaged using Fisher statistics. For intensities, the process was identical but rather used a normal distribution with the reported standard deviation of the estimate.
d. The simulated site-mean direction or intensity was then converted to a VGP or VADM.

After steps 3a. to 3d. were complete for the whole of both datasets, the median simulated VGP colatitude and the median and IQR of the simulated VADMs were then calculated. These provide plausible values for the proxy that would be obtained if the field was behaving the same as in the simulation, given the sampling distribution and measurement errors associated with the real dataset.

https://doi.org/10.5194/egusphere-2025-5616
Preprint. Discussion started: 20 November 2025

Step 4: Constructed bespoke proxy plots for three SHAnalogues. Step 3 was repeated 200 times for each of the geodynamo simulations and all of the resulting simulated proxies were plotted against the associated "true" SHAnalogues (ADF_{median}, *Roughness,* and *Volatility*). Since each simulated proxy (plotted on the x-axis) is calculated using a finite number of different randomly obtained timesteps whereas the corresponding SHAnalogue (plotted on the y-axis) is a single value derived from all timesteps, the resulting points fell on horizontal lines as shown for the 0.1-1 Ma bespoke proxy plots in figure 2(a-c). Each line represents a range of plausible proxies that a field, defined by the single SHAnalogue, could produce under the specific sampling conditions given.

Step 5: Estimated SHAnalogues for the time interval. A linear regression provided the best-fit relationship between each simulated proxy and the corresponding SHAnalogue allowing the observed proxies to be converted into ADF_{median}, *Roughness*, and *Volatility* as illustrated for 0.1-1 Ma in figure 2(a-c). Uncertainties associated with both the observed proxy values and the best-fitting relationships require combining but the optimal approach for doing this was not immediately clear. Although 95% uncertainties were calculated for both, simply using the intersections of these produced combined uncertainties (effectively at the 99.975% confidence level) that were overly conservative. Furthermore, the bespoke proxy plots tended to splay out at higher values leading to further overestimation of the uncertainty when the observed proxy had a low value. Various approaches were trialled through analysing the results of the validation tests that are outlined below. The optimal approach for defining uncertainty on each of the

https://doi.org/10.5194/egusphere-2025-5616
Preprint. Discussion started: 20 November 2025

SHAnalogues was determined to be a Monte Carlo method that combined the bootstrapped observed proxy values, the uncertainty on the linear fit, and random scatter calculated from the residuals of the points around the best fit. Only points on the plot that were from simulations which produced more than 1% of their proxy values below the upper 95% confidence bound of the observed proxy (shown in bold on figure 2a-c) were included in the calculation. This produced 10,000 bootstraps of each SHAnalogue from which 95% confidence bounds were calculated.

It follows that:

$$NADF_{median} = ADF_{median}.Roughness^2 \quad (6)$$

Uncertainties of $NADF_{median}$ were defined by coupling the bootstraps already obtained for $NADF_{median}$ and *Roughness*.

Step 6: Performed validation checks. The accuracy of the estimated SHAnalogues was independently tested using synthetic palaeomagnetic datasets drawn from each of 11 geomagnetic field models (Table S1). The datasets were generated, once more, by following the spatial distribution of the palaeomagnetic observations, drawing randomly in time, and adding appropriate random noise. All of the above steps were then followed using the synthetic datasets in place of the actual data. This allowed uncertainty bounded-SHAnalogues to be estimated for each of the field models and to be compared to the respective known SHAnalogue value (figures 2d-g). Tuning of the uncertainty estimation process (see step 5) was performed to ensure that all

https://doi.org/10.5194/egusphere-2025-5616
Preprint. Discussion started: 20 November 2025

44 tests performed on the 0.1-1 Ma data distributions produced estimates that encompassed the true SHAnalogue within their 95% confidence bounds while not being overly conservative.

A fundamental assumption of the whole approach outlined above is that the geodynamo simulations used in the SHAnalogue estimation produce field behaviours that are sufficiently relevant to the Earth to enable the relationships between the measured proxies and the palaeomagnetic SHAnalogues to be constrained reliably. The points in figure 2d-g are derived from independent geomagnetic field models generated in a radically different way to the simulated fields output from the ensemble. Their proximities to the one-to-one lines support that this assumption is reasonable.

3. Characteristics of the 0-15 Ma palaeomagnetic field

Steps 1 to 6 were repeated for intervals 1-4 Ma and 4-15 Ma. Datasets were compiled using the same sources and selection criteria (Step 1 above). The palaeosecular variation dataset for the Miocene (PSVM; Engbers *et al.*, 2022) was integrated with PSV10-24 to supply palaeomagnetic directions for the earliest interval. Results are summarised in figure 3 and table 1 with distributions of 1-15 Ma data, bespoke proxy plots, and independent test results shown in figures S6-S9. The same method for estimating uncertainties as developed for 0.1-1 Ma was applied to the earlier intervals and validation tests supported the accuracy of the estimated SHAnalogues. While not every test passed (table 1), success rates across the three intervals was in line with the

https://doi.org/10.5194/egusphere-2025-5616
Preprint. Discussion started: 20 November 2025

expectation of 95% and the failures that did occur were marginal. In the discussion below, SHAnalogues estimated from two intervals were judged as being indistinguishable if the 95% confidence bounds from either overlapped with the central estimate from the other.

<Figure 3>

<Table 1>

Estimates of both ADF_{median} and $NADF_{median}$ were distinctly high for 0.1-1.0 Ma relative to the two earlier time periods (figure 3a; table 1). *Roughness* estimates, by contrast, fall in a narrow range such that, even given the small uncertainties related to the large number of directional data (table 1), only the 1-4 Ma and 4-15 Ma intervals were marginally distinguishable (figure 3b). The spread for *Volatility* estimates was somewhat larger with the central values appearing to increase with age but the uncertainties were also somewhat elevated. Considering these, the estimate for 0.1-1 Ma is marginally distinguishable from the substantially higher *Volatility* estimate obtained for 4-15 Ma.

Values of ADF_{median} obtained from the palaeomagnetic datasets and time-varying geomagnetic field models (all of which are derived from 0-1 Ma) strongly suggest that the geomagnetic field has, in the last million years, supported an axial dipole that is high on average compared to the preceding 14 million years (figure 3a). Caution should be employed in interpreting this as a strengthening trend since the reduced temporal resolution with increasing age prevents the identification of similar length intervals earlier in the last 15 million years. Differences in the

https://doi.org/10.5194/egusphere-2025-5616
Preprint. Discussion started: 20 November 2025

nonaxial dipole field are slightly less clear; $NADF_{median}$ from time-varying models are intermediate between the values estimated for 0.1-1 Ma and the earlier intervals. Only values of *Roughness* derived from time-varying field models LSMOD and GGFMB, that are focused specifically on intervals of instability, are in the range of the palaeomagnetic datasets; the others are lower (figure 3b). All values of *Volatility* from time-varying models are lower than those derived from palaeomagnetic datasets. It seems likely that the regularisation employed in the generation of the time-varying field models causes at least some underestimation of all SHAnalogues except ADF_{median}.

GGP models do not employ regularisation but, being derived directly from palaeomagnetic datasets, may be biased by distributions being nonuniform in both space and time. Spatial inhomogeneity is dealt with directly in the new SHAnalogue estimation process outlined here through downsampling. Similarly, the risk of bias from temporal inhomogeneity is somewhat mitigated by the choice of intervals made which avoids the age distributions within them being strongly skewed (see figures S5c,d; S6c,d; S7c,d).

SHAnalogues provide robust measures of palaeomagnetic field behaviour but it is worth considering their relation to the extremes represented by polarity reversals since the occurrence of these is very well documented over the last 15 million years (Ogg, 2012). It has long been hypothesised that strong fields may inhibit the occurrence of reversals (Cox, 1968); differences in average rates of reversal occurrence and ADF_{median} in the three intervals studied here appear to

https://doi.org/10.5194/egusphere-2025-5616
Preprint. Discussion started: 20 November 2025

support this (figure 3c). Since the axial dipole field must reach zero for a reversal to occur, it seems intuitive that estimates of *Volatility* also appear to increase with reversal occurrence. Interestingly however, the observed differences in *Volatility* may be entirely explained by associated shifts in ADF_{median}. The absolute variance of the total field can be calculated:

$$TF_{iqr} = Volatility^2 . ADF_{median} \quad (7)$$

This value appears, large uncertainties notwithstanding, to have remained remarkably constant (~15-17 μT) across the three intervals with differing average reversal frequencies (figure 3d).

The robustness of all observations made above were tested by repeating the entire process after removing the 29% of palaeointensity data that did not comprise measurements made using the Thellier method with pTRM checks (figure S10). Values of ADF_{median} and $NADF_{median}$ from each interval were largely unchanged while *Volatility* decreased in all three intervals and especially for 4-15 Ma (from 0.95 to 0.85). Values of TF_{iqr} decreased only marginally (to ~ 15 μT) and became even more consistent across intervals (figure S10d). While values of TF_{median} and ADF_{iqr} are not directly estimable from SHAnalogues, Table S1 suggests they should be very similar to ADF_{median} and TF_{iqr} respectively.

SHAnalogues calculated across the 0-15 Ma interval support suggestions that ~1 million years may not be sufficient to produce converged estimates of the time-averaged field strength (Davies and Constable, 2014) and that the field in the Bruhnes may have been anomalously strong relative to the longer term average. This argument has been made previously using absolute

https://doi.org/10.5194/egusphere-2025-5616
Preprint. Discussion started: 20 November 2025

(Chen *et al.*, 2025, Tauxe, 2006) and relative (Valet *et al.*, 2024, Valet *et al.*, 2005) palaeointensities but was countered recently by Buffett and Avery (2025). A new claim here is that the absolute variance of the field strength may have showed little change across the three periods. If the variance within all three intervals mostly reflects fluctuations on timescales < 1 million years, and the average axial dipole was indeed far above zero in the last million years, then if follows that reversals should have become less common. Using data from much earlier intervals, previous studies have suggested that the average and variance of the dipole moment are positively correlated to one another and to (average) chron length (Biggin and Thomas, 2003, Tauxe and Staudigel, 2004). The variance in field strength in 0-15 Ma appears not be strongly correlated to either (figure 3d); this allows long chrons such as the Bruhnes to be explained as the likely outcome of extended intervals of elevated axial dipole.

SHAnalogues provide a framework for describing global properties of the palaeomagnetic field in a robust manner that accounts for uneven spatial distributions of data and measurement errors. They have clear potential for constraining statistical models of palaeomagnetic field behaviour and simulations of the geodynamo process on long timescales. While they currently cover fewer aspects of palaeomagnetic behaviour than the parameters used in Q_{PM} criteria (Sprain *et al.*, 2019) which also provide benchmarks, they are much easier to calculate from model outputs and may be less prone to the influence of outliers and inhomogeneous distributions. It is suggested that geodynamo simulations aiming to capture recent palaeomagnetic field behaviour should output *Roughness* and *Volatility* values within errors of those from both the 1-4 Ma and 4-15 Ma

https://doi.org/10.5194/egusphere-2025-5616
Preprint. Discussion started: 20 November 2025

intervals. Some 7 simulations from the ensemble achieve this and amongst these are two which have the smallest measured Q_{PM} misfit values of all considered here (table S1). Yielding all four SHAnalogues within the range of those from 1-15 Ma may be considered a desirable target for future GGP models too.

There is a great deal of scope to develop SHAnalogues and their applications in the future. The addition of further parameters, e.g. addressing the field's time-averaged morphology and proneness to extreme behaviour, will allow a more comprehensive characterisation of the palaeomagnetic field than performed here. Moreover, the estimation process itself could be augmented to deal with temporally non-uniform datasets and uncertainties in palaeogeographical reconstructions (used for relocation of the datasets). Doing so will be particularly useful in allowing SHAnalogues to be estimated for earlier geological periods where their capacity for generating further insights into palaeomagnetic field behaviour will potentially be very significant.

Data Availability Statement

All palaeomagnetic directions are available on the MagIC database (www. earthref.org/MagIC/) under the following doi's:

http://dx.doi.org/10.7288/V4/MAGIC/20079;

http://dx.doi.org/10.7288/V4/MAGIC/19609;

https://doi.org/10.5194/egusphere-2025-5616
Preprint. Discussion started: 20 November 2025

The palaeointensity data were taken from PINTv8.2.0 at http://www.pintdb.org

Both compiled datasets with reconstructed locations and rotated declinations are provided as Supplementary Datasets 1 and 2.

Code to generate SHAnalogues and associated parameters are available from: https://github.com/andybiggin/Public/tree/a4702a19a7d84474b5279c68539b4016480b4069/CalculateSHAnalogues [Note: this folder will be posted on EarthRef upon acceptance].

Acknowledgements

Brendan Cych, Chris Davies, Thomas Frasson, Richard Holme, Simon Lloyd, Mary Murray and Greig Paterson are thanked for discussions during the development of this work.

References

Biggin, A.J., Bono, R.K., Meduri, D.G., Sprain, C.J., Davies, C., Holme, R. & Doubrovine, P.V., 2020. Quantitative estimates of average geomagnetic axial dipole dominance in deep geological time, *Nat Commun,* 11**,** 6100.

Biggin, A.J., Davies, C., Mound, J., Lloyd, S.J., Engbers, Y.A., Thallner, D., Clarke, A. & Bono, R.K., 2025. Heterogeneity in core-mantle heat flow influenced the ancient geodynamo, *Nat Geosci,* In Revision.

Biggin, A.J. & Paterson, G.A., 2014. A new set of qualitative reliability criteria to aid inferences on palaeomagnetic dipole moment variations through geological time, *Frontiers in Earth Science,* 2**,** 24, 21-29.

Biggin, A.J. & Thomas, D.N., 2003. Analysis of long-term variations in the geomagnetic poloidal field intensity and evaluation of their relationship with global geodynamics, *Geophys J Int,* 152**,** 392-415.

https://doi.org/10.5194/egusphere-2025-5616
Preprint. Discussion started: 20 November 2025

Bono, R.K., Biggin, A.J., Holme, R., Davies, C., Meduri, D.G. & Bestard, J., 2020. Covariant Giant Gaussian Process Models with Improved Reproduction of Palaeosecular Variation, *Geochem Geophy Geosy,* 21**,** e2020GC008960.

Bono, R.K., Paterson, G. & Biggin, A., 2022. MCADAM: A continuous paleomagnetic dipole moment model for at least 3.7 billion years, *Geophys Res Lett,* 49**,** e2022GL100898.

Brown, M.C., Korte, M., Holme, R., Wardinski, I. & Gunnarson, S., 2018. Earth's magnetic field is probably not reversing, *P Natl Acad Sci USA,* 115**,** 5111-5116.

Buffett, B. & Avery, M., 2025. Quantifying Uncertainty in Time Averages of the Geomagnetic Dipole, *Geophys Res Lett,* 52**,** e2025GL118741.

Chen, X., Biggin, A.J. & Lloyd, S.J., 2025. Stabilisation of full-vector palaeosecular variation in the last 5 million years: Insights from a newly updated Palaeointensity (PINT) Database, *Geophys J Int,* Submitted.

Cox, A., 1968. Lengths of geomagnetic polarity intervals, *Journal of Geophysical Research (1896-1977),* 73**,** 3247-3260.

Davies, C. & Constable, C., 2014. Insights from geodynamo simulations into long-term geomagnetic field behaviour, *Earth Planet Sc Lett,* 404**,** 238-249.

Engbers, Y.A., Bono, R.K. & Biggin, A.J., 2022. PSVM: A global database for the Miocene indicating elevated paleosecular variation relative to the last 10 Myrs, *Geophys J Int,* 23**,** e2022GC010480.

Mahgoub, A.N., Korte, M. & Panovska, S., 2023. Global Geomagnetic Field Evolution From 900 to 700 ka Including the Matuyama-Brunhes Reversal, *Journal of Geophysical Research: Solid Earth,* 128**,** e2023JB026593.

Meduri, D.G., Biggin, A.J., Davies, C., Bono, R.K., Sprain, C.J. & Wicht, J., 2021. Numerical geodynamo simulations reproduce palaeomagnetic field behaviour, *Geophys Res Lett,* 48**,** e2020GL090544.

Mound, J.E. & Davies, C.J., 2023. Longitudinal structure of Earth's magnetic field controlled by lower mantle heat flow, *Nat Geosci,* 16**,** 380-385.

Müller, R.D., Zahirovic, S., Williams, S.E., Cannon, J., Seton, M., Bower, D.J., Tetley, M.G., Heine, C., Le Breton, E., Liu, S., Russell, S.H.J., Yang, T., Leonard, J. & Gurnis, M., 2019. A Global Plate Model Including Lithospheric Deformation Along Major Rifts and Orogens Since the Triassic, *Tectonics,* 38**,** 1884-1907.

Nilsson, A., Suttie, N., Stoner, J.S. & Muscheler, R., 2022. Recurrent ancient geomagnetic field anomalies shed light on future evolution of the South Atlantic Anomaly, *Proceedings of the National Academy of Sciences,* 119**,** e2200749119.

Ogg, J.G., 2012. Geomagnetic Polarity Time Scale. *in The Geologic Time Scale 2012*, pp. 85-113.

Panovska, S., Constable, C. & Korte, M., 2018. Extending Global Continuous Geomagnetic Field Reconstructions on Timescales Beyond Human Civilization, *Geochem Geophy Geosy,* 19**,** 4757-4772.

https://doi.org/10.5194/egusphere-2025-5616
Preprint. Discussion started: 20 November 2025

Panovska, S., Korte, M., Liu, J. & Nowaczyk, N., 2021. Global Evolution and Dynamics of the Geomagnetic Field in the 15–70 kyr Period Based on Selected Paleomagnetic Sediment Records, *Journal of Geophysical Research: Solid Earth,* 126, e2021JB022681.

Pavon-Carrasco, F.J., Osete, M.L., Torta, J.M. & De Santis, A., 2014. A geomagnetic field model for the Holocene based on archaeomagnetic and lava flow data, *Earth Planet Sc Lett,* 388, 98-109.

Schanner, M., Korte, M. & Holschneider, M., 2022. ArchKalmag14k: A Kalman-Filter Based Global Geomagnetic Model for the Holocene, *Journal of Geophysical Research: Solid Earth,* 127.

Sprain, C.J., Biggin, A.J., Davies, C.J., Bono, R.K. & Meduri, D.G., 2019. An assessment of long duration geodynamo simulations using new paleomagnetic modeling criteria (QPM), *Earth Planet Sc Lett,* 526, 115758.

Stacey, F.D., 1992. *Physics of the Earth* 3rd edn, Vol., pp. Pages, Brookfield Press.

Tauxe, L., 2006. Long-term trends in paleointensity: The contribution of DSDP/ODP submarine basaltic glass collections, *Phys Earth Planet In,* 156, 223-241.

Tauxe, L., Heslop, D. & Gilder, S.A., 2024. Assessing Paleosecular Variation Averaging and Correcting Paleomagnetic Inclination Shallowing, *Journal of Geophysical Research: Solid Earth,* 129, e2024JB029502.

Tauxe, L. & Kent, D.V., 2004. A simplified statistical model for the geomagnetic field and the detection of shallow bias in paleomagnetic inclinations: was the ancient magnetic field dipolar?, *AGU Geophysical Monograph Series,* 145, 101-115.

Tauxe, L. & Staudigel, H., 2004. Strength of the geomagnetic field in the Cretaceous Normal Superchron: New data from submarine basaltic glass of the Troodos Ophiolite, *Geochem Geophy Geosy,* 5, Art. No. Q02H06.

Valet, J.-P., Savranskaia, T., Egli, R., Simon, Q., Bassinot, F. & Thouveny, N., 2024. Beryllium ten production and relative paleointensity for the past 1.2 million years, *Quaternary Sci Rev,* 344, 108993.

Valet, J.P., Meynadier, L. & Guyodo, Y., 2005. Geomagnetic dipole strength and reversal rate over the past two million years, *Nature,* 435, 802-805.

Ziegler, L.B., Constable, C.G., Johnson, C.L. & Tauxe, L., 2011. PADM2M: a penalized maximum likelihood model of the 0-2 Ma palaeomagnetic axial dipole moment, *Geophys J Int,* 184, 1069-1089.

https://doi.org/10.5194/egusphere-2025-5616
Preprint. Discussion started: 20 November 2025

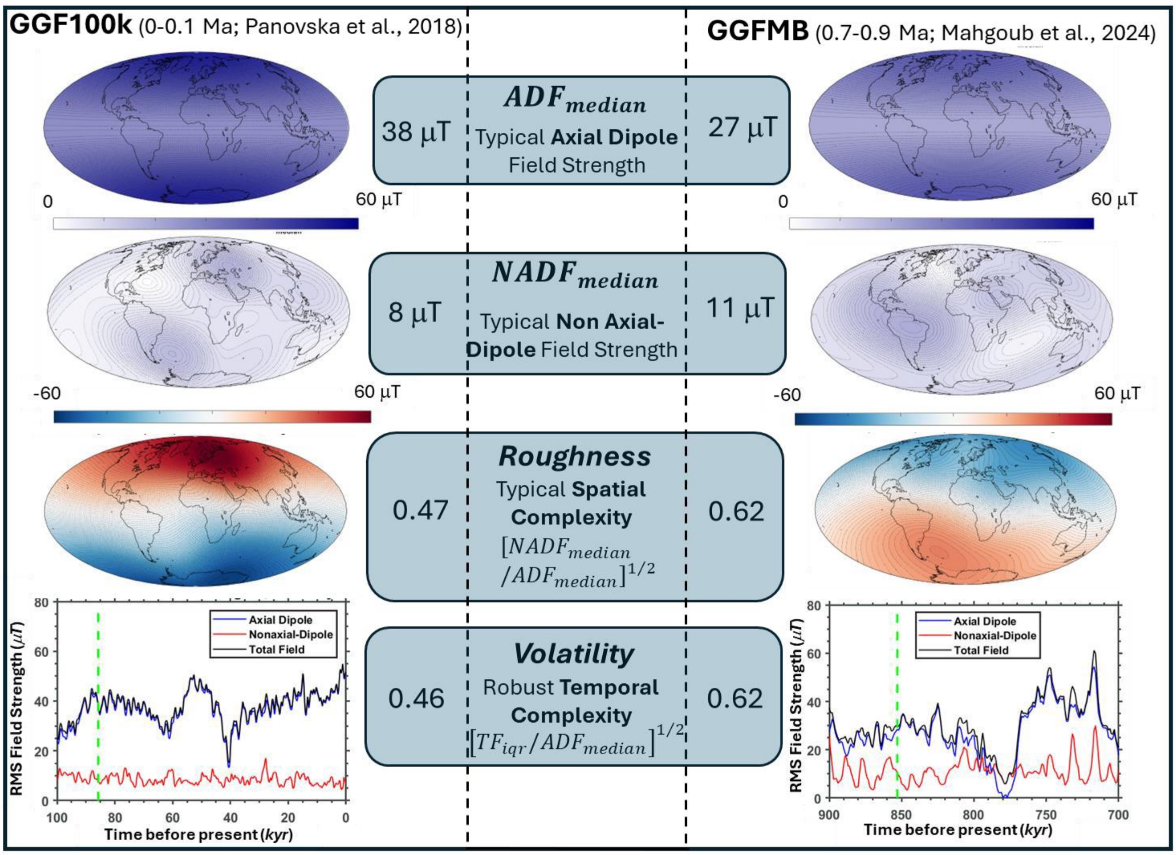

Figure 1: Spherical Harmonic Analogues illustrated using two recent-field models. Maps in the top row show field strength produced by the axial dipole (g_1^0 term). Maps in the second row show field strength from the nonaxial-dipole field (all other terms). Maps in the third row show the radial component of the total field. The bottom row shows time series of the RMS field strength of the axial dipole, nonaxial-dipole, and total fields. The maps are drawn from representative time instances shown by the green dashed line in the bottom row and are truncated to degree and order 10.

https://doi.org/10.5194/egusphere-2025-5616
Preprint. Discussion started: 20 November 2025

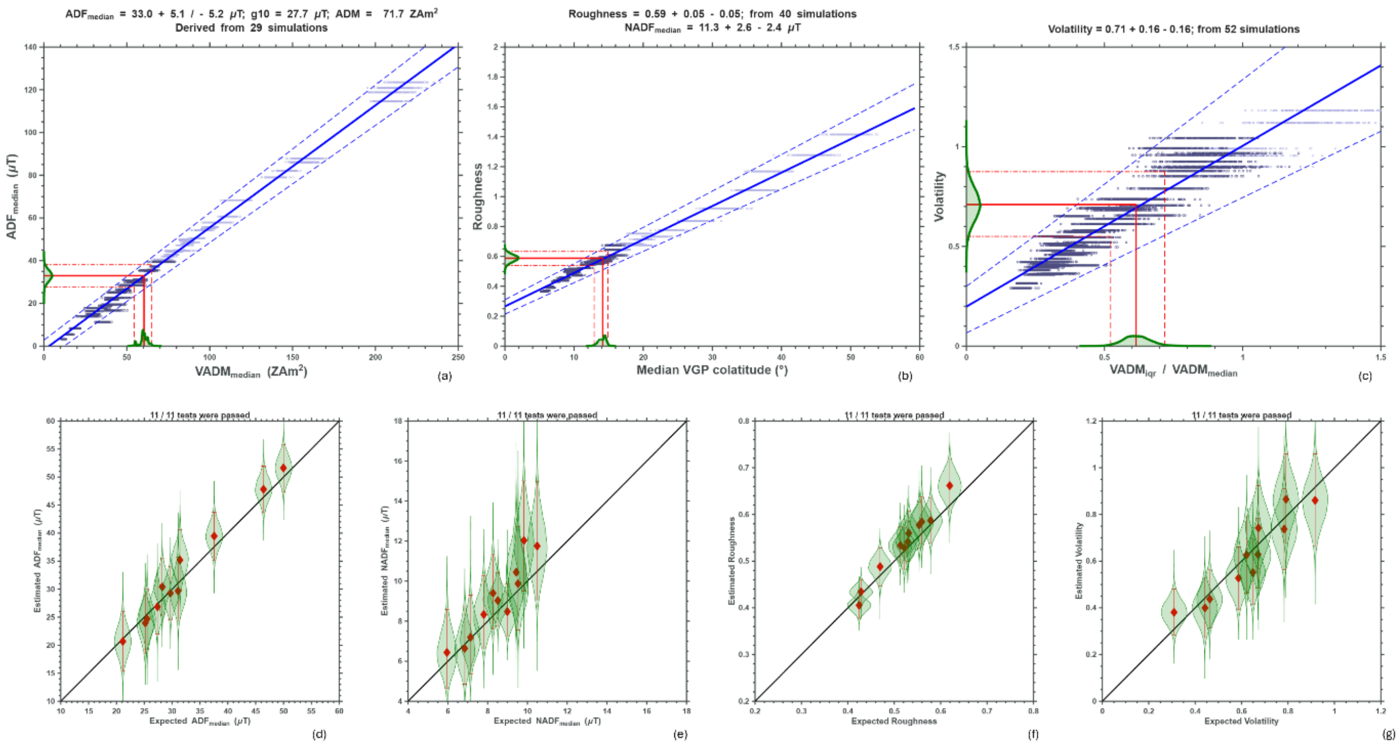

Figure 2: SHAnalogue estimation and testing for the 0.1-1 Ma time interval. (a-c): Bespoke proxy plots derived from outputs of geodynamo simulations down-sampled randomly in time at the spatial resolution of the palaeomagnetic datasets. Each horizontal row of blue points represents 200 proxy values (plotted on x-axis) calculated from a simulation with a single "true" SHAnalogue value (plotted on y-axis). Darker coloured points were used in the estimation of the SHAnalogues from the palaeomagnetic proxies. Vertical red lines indicate the palaeomagnetic proxy central values (solid) and 95% uncertainties (dashed). Horizontal red lines are the corresponding palaeomagnetic SHAnalogue estimates (see text for details of calculation). The shapes of the distributions (amplitudes are arbitrary) of both are shown in green. (d-g) One-to-one plots of the expected and estimated SHAnalogues obtained after down-sampling the 11 geomagnetic field models at the resolution of the 0.1-1 Ma datasets and subjecting these synthetic measurements to the same process as shown in upper panels. The estimates and 95% uncertainties are shown in red while violin plots in green show the shapes of the distributions using arbitrary, relative amplitudes.

https://doi.org/10.5194/egusphere-2025-5616
Preprint. Discussion started: 20 November 2025

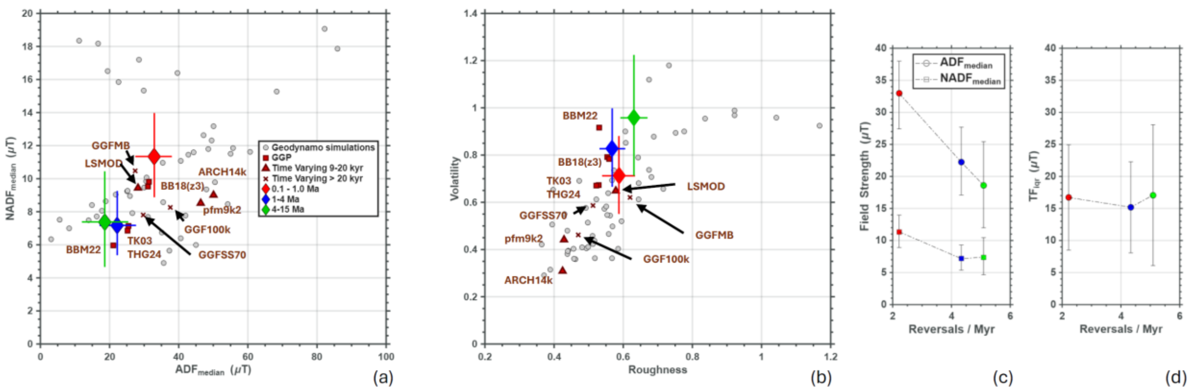

Figure 3: Summary of SHAnalogue estimation and averaged polarity reversal frequency for the time periods 0.1-1 Ma, 1-4 Ma, and 4-15 Ma. (a,b) Plot of ADF_{median} vs. $NADF_{median}$ and *Roughness* vs. *Volatility* with direct measurements from geomagnetic field models and geodynamo simulations also shown. (c) Plots of ADF_{median} and $NADF_{median}$ vs. polarity reversal rate. (d) Plot of TF_{iqr} (derived from $Volatility^2$. ADF_{median}) vs. polarity reversal rate. All error bars indicate 95% uncertainty bounds

https://doi.org/10.5194/egusphere-2025-5616
Preprint. Discussion started: 20 November 2025

Time period	N_{dir}	N_{int}	ADF_{median} (μT)	$NADF_{median}$ (μT)	*Roughness*	*Volatility*	Test Success
0.1-1 Ma	544	190	33 + 5 / -6	11 ± 3	0.59 ± 0.05	0.71 + 0.17 /-0.16	100%
1-4 Ma	796	270	22 ± 5	7 ± 2	0.57 ± 0.04	0.83 ± 0.17	91%
4-15 Ma	870	111	19 + 7 / -6	7 ± 3	0.63 ± 0.04	0.95 + 0.26 /-0.24	98%

436 **Table 1:** Summary of SHAnalogue estimation from palaeomagnetic datasets